JOURNAL GEOLOGICAL SOCIETY OF INDIA
Vol.89, January 2017, pp.77-81

# An Insight into Slope Stability Using Strength Reduction Technique

V. B. Maji
Department of Civil Engineering, Indian Institute of Technology Madras, Chennai - 600 036, India
*E-mail: vbmaji@gmail.com*

## ABSTRACT

**In Shear strength reduction (SSR) technique, the factor of safety (FOS) is defined as the ratio of the material's actual shear strength to the minimum shear strength required to prevent failure. Failure surface is found automatically through the zones within the material, where applied shear stresses cross the shear strength of the material. In this paper, a review of the technique is discussed in reference to *FLAC*. A brief background of the approach together with detailed procedure is presented. An attempt is made to exhibit the shear strength dependency of the strain. As stability of the slope is a function of the shear strength, the development of failure strain reflects the potential failure zone of slope. The shear strain developed in the slope increases with reduction in the shear strength and is reflected in the analysis. The concept of failure ratio ($R_f$) is incorporated in shear strength reduction technique and is demonstrated. Relationships between the critical shear strength reduction ratio and the safety factor are examined.**

## INTRODUCTION

Slope stability analysis using shear strength reduction (SSR) technique is widely accepted these days because of increasing computing power and resources available to the geotechnical engineers. In this method, the factor of safety (FOS) is defined as the ratio of the material's actual shear strength to the minimum shear strength required to prevent failure. As it is also known from the shear strength reduction factor, one can compute FOS with finite element/finite difference methods by reducing the shear strength until failure occurs. The critical factor at which failure occurs, is taken to be the FOS. The concept of shear strength reduction technique is not very old and was first used by Zienkiewiez et al. (1975) and later been applied by Naylor (1982), Donald & Giam (1988), Matsui & Sun (1992), Ugai (1989), Ugai & Leshchinsky (1995), Dawson et al. (1999), Griffith and Lane (1999), Cala & Flisiak, (2003), Zheng et al. (2005), Cheng (2007), Zheng et al. (2009), Kainthola et al. (2012), Singh et al. (2013) and others. Dawson et al. (1999) compared the slope stability factor computed with strength reduction technique with upper bound limit analysis solution based on log spiral failure mechanism. Recently Cheng (2007) compared the FOS and the location of critical failure surfaces obtained by the limit equilibrium and SSR method.

There are many advantages of shear strength reduction technique over limit equilibrium analysis. The usual difficulty with all the equilibrium methods is, they are based on the assumption that the failing mass can be divided into slices. This in turn necessitates further assumptions relating to side force directions between slices, with consequent implications for equilibrium (Griffiths & Lane, 1999). The assumption made about the side forces is one of the main characteristics that artificially distinguish one limit equilibrium method from another. In the shear strength reduction method, no assumption needs to be made in advance about the shape or location of the failure surface. Here, the failure surface is found automatically through the zones within the material where applied shear stresses cross the shear strength of the material. As there is no concept of slices, there is no need for assumptions about inter slice side forces. SSR is applicable to many complex conditions and can give information such as stresses and movements and pore pressures which are not possible with the LEM (Cheng et al. 2007). Use of appropriate constitutive model and parameters, boundary conditions and the definition of failure condition/ failure surface are the key aspects to be considered in SSR method (Cheng et. al, 2007).

The FOS obtained from SSR is usually the same as FOS obtained from limit equilibrium method (LEM) (Griffiths & Lane, 1999; Dawson et al., 1999, Cala & Flisiak, 2003) and usually within a few percent of the limit analysis solution provided that sufficiently refined numerical mesh adopted (Fig.1). SSR values are generally slightly higher side as compared to LEM predictions. For complex geology slopes, there may be considerable difference between FOS values from SSR and LEM (Cala & Flisiak, 2003). Slope stability analysis by SSR is accurate, robust and simple enough for routine use. Easy implementation of SSR with computer programs and their graphical capabilities also allow better understanding of the mechanisms of failure. Application of the technique has been limited in the past due to the long computational run times required. With the increased speed of PCs, the technique has become very common in comparison with the method of slices, and is being used increasingly in engineering practice. There are number of commercial software programs available for SSR analysis like *FLAC* and *PLAXIS*, which are widely used for the slope stability analysis. A detailed investigation on the slope stability analysis using SSR technique is discussed here.

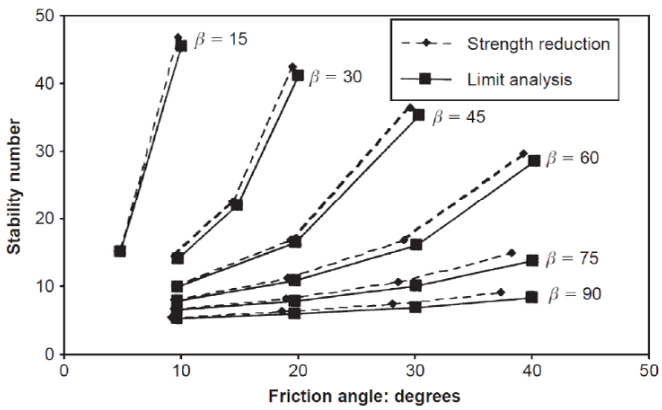


**Fig.1.** Comparison of Strength reduction and limit analysis stability numbers for slopes with inclination β (Dawson et al., 1999)

## FACTOR OF SAFETY (FOS) WITH SSR

FOS can be calculated automatically based on strength reduction technique that performs a series of simulations while changing the strength properties to determine the condition at which an unstable state exists. The FOS is found corresponding to the point of instability, and the critical failure surface is located in the model. To perform slope stability analysis with the shear strength reduction technique, simulations are run for a series of trial factor of safety $F_{trial}$ with, $c$ and $\phi$ adjusted according to following equations,

$$c^{trial} = \frac{1}{F^{trial}} c \tag{1}$$

$$\phi^{trial} = \tan^{-1}\left[\frac{1}{F^{trial}} \tan\phi\right] \tag{2}$$

The value of $F_{trial}$ at which slope fails is found efficiently in *FLAC* using bracketing and bisection method. In the bracketing and bisection techniques, first upper and lower brackets are established. The initial lower bracket is any $F_{\mathrm{trial}}$ for which a simulation converges. The initial upper bracket is any $F_{\mathrm{trial}}$ for which the simulation does not converge. Next, a point midway between the upper and lower brackets is tested. If the simulation converges, lower bracket is replaced by this new value. If the simulation does not converge, the upper bracket is replaced. The process is repeated until the difference between upper and lower brackets is less than a specific tolerance. When the calculation is complete, the final value is reported.

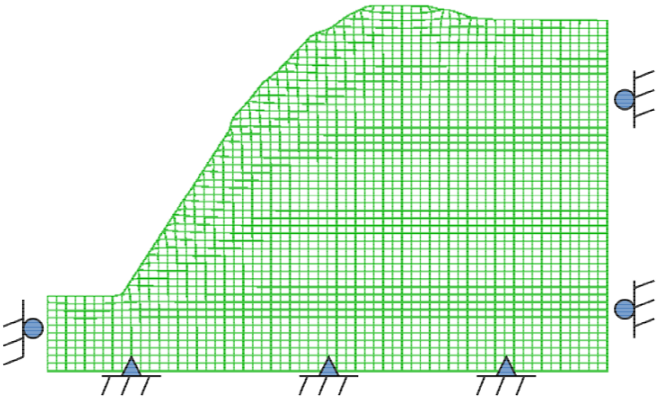

**Fig.2.** Mesh generated for the natural slope using *FLAC*

The finite difference mesh for a generalized large scale natural slope in rockmass is considered as an example to demonstrate the slope stability analysis using *FLAC* (Fig.2). The slope mesh, 1 is 60 zones wide and 50 zones high. Horizontal displacements are fixed for nodes along the left and right boundaries while both horizontal and vertical displacements are fixed along the bottom boundary. Table 1, gives the Mohr-Coulomb material properties used for the present slope stability analysis. Slope stability with SSR technique usually recommends single values for Young's modulus and Poisson's ratio for slope material and supports assumption of zero dilation angles. Modulus values, Poisson's ratio and dilation angle influence the magnitude of the computed deformations and therefore right estimates of these properties is required. Figure 3a shows the maximum shear strain rate for the slope in example along with velocity vectors. In this example, failure surface is almost circular from top of the slope to the toe. Figure 3b shows the plasticity indicator plot of the same slope.

**Table 1.** Mohr-Coulomb material properties used for the model

| Material Parameters | Values |
|---|---|
| Cohesion | 546 kPa |
| Friction angle | 22° |
| Bulk modulus | 1.5 GPa |
| Shear Modulus | 1.2 GPa |
| Density | 2700 kg/m$^3$ |

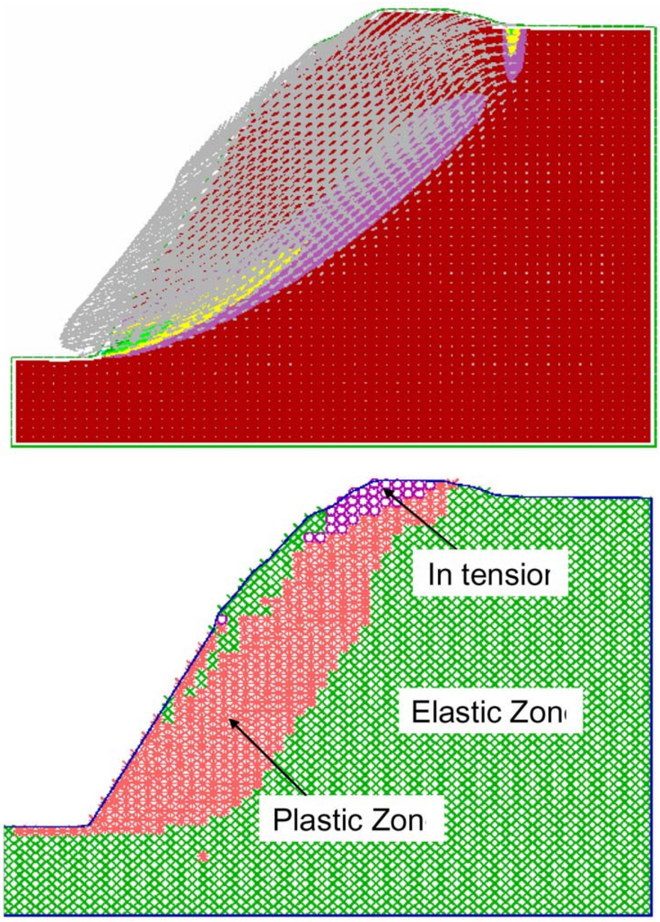


**Fig.3. (a)** Critical failure surface. **(b)** Plasticity indicator plot depicting the various zones.

They reveal those zones in which the stresses satisfy the yield criterion. A failure indicated by the contiguous line of active plastic zones that join two surfaces. It has been observed in this particular case that the initial plastic flow occurred at the beginning of the simulation but subsequent to stress redistribution, the yielding elements are unloaded. The active yielded elements failed in tension and are important to the detection of a failure mechanism. The yielded zone due to shear can be seen in the Fig.3b and as observed, it also follows a circular failure surface.

## DEFINITION OF FAILURE

There are several possible definitions of failures for different methods but usually slope failure and numerical non-convergence occur simultaneously. In *FLAC*, the failure of the slope can be understood through the total unbalance force, which is the algebraic sum of the total force in a grid point. For a failed slope the solution will not converge and hence the program stepping will not stop (representing infinite solution). If the slope is stable then the stepping will automatically stop when the total unbalance force reaches zero or below a set limit. Figure 4 shows the variation of maximum unbalanced force with time step. Figure 4a representing the slope to be stable where, minimization of unbalance force can be seen at around 1400 steps and after that the stepping stops automatically i.e. solution converges. Figure 4b shows the maximum unbalance force plot with steps where stepping continues even after 5000 steps but the solution doesn't converge representing a failed slope.

Dawson et al. (1999) showed that, there is a sharp break (Fig.5) in the unbalanced force when the trial factor of safety reaches a certain critical value for elastic perfectly plastic model. Therefore, there is no ambiguity in finding the trial FOS at which slope fails. But

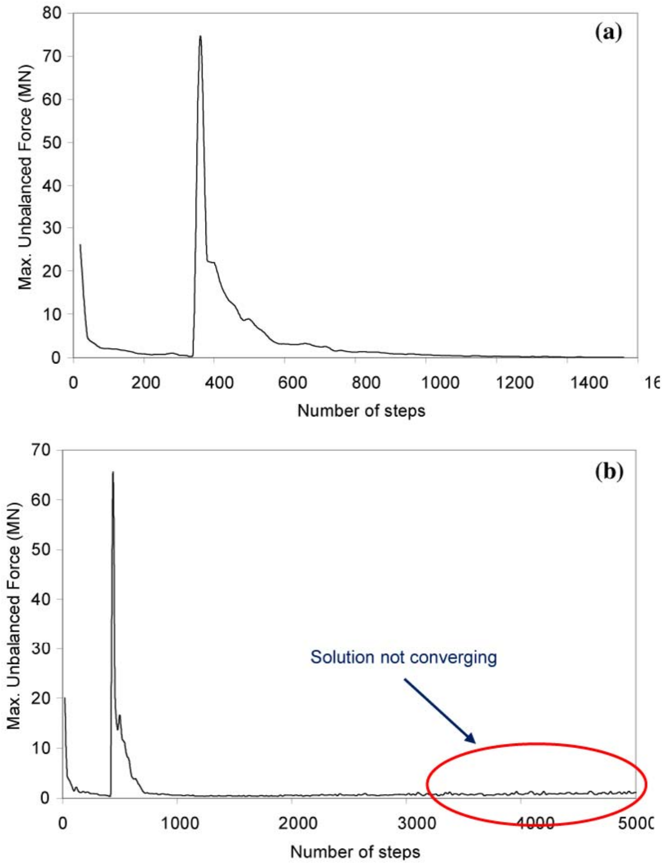

**Fig.4.** Maximum unbalanced force with steps **(a)** Solution converges **(b)** Solution does not converge

for constitutive models where, there are smooth changes in elastic to plastic behaviour like hyperbolic model (Duncan and Chang, 1970), identifying the limiting state may be difficult. Table 2 presents the factor of safety (FOS) values obtained from the manual reduction of shear parameters. It is to be noted though obvious, that the value of FOS for the manual reduction factor 1.2 is 1, which intern represents the FOS.

## SHEAR STRENGTH DEPENDENCY OF THE STRAIN

An attempt is also made to exhibit the shear strength dependency of the strain through the hyperbolic stress-strain model using *FLAC*. Stability of the slope is a function of the shear strength and the development of failure strain reflecting the potential failure zone of slope. The shear strain developed in the slope increases with reduction in the shear strength. The concept of failure ratio is incorporated in shear strength reduction technique and is applied to a large scale natural slope. Relationships between the critical shear strength reduction ratio and the safety factor are examined. The shear strain developed in the slope increases with reducing the shear strength. The relationship

**Table 2.** Values of FOS for trial manual reduction values

| Reduction Factor | 'c' kPa | 'ϕ' (º) | FOS |
|---|---|---|---|
| 0.9 | 606 | 24 | 1.33 |
| **1** | **546** | **22** | **1.2** |
| 1.1 | 496 | 20 | 1.09 |
| 1.14 | 479 | 19.5 | 1.05 |
| 1.16 | 470 | 19.2 | 1.03 |
| 1.18 | 462 | 18.9 | 1.02 |
| 1.19 | 458 | 18.7 | 1.01 |
| **1.2** | **455** | **18.6** | **1.00** |
| 1.5 | 364 | 15 | 0.8 |
| 1.6 | 341 | 14 | 0.75 |

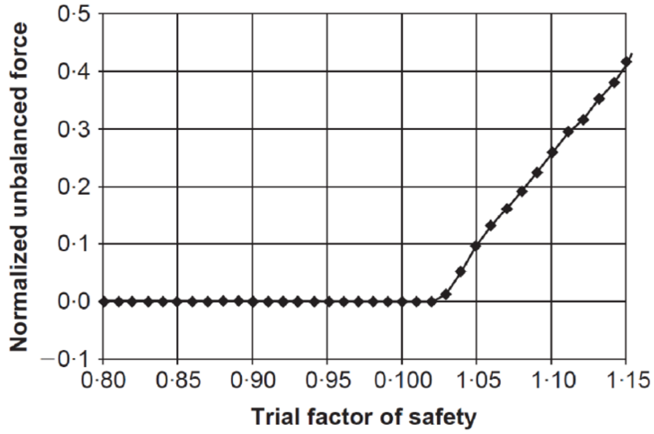

**Fig.5.** Unbalanced force as the trial factor of safety is increased in small steps (Dawson et al., 1999).

between the shear strength reduction ratio and shear strain for different values of failure ratio ($R_f$) is studied. It is observed that, the value of shear strain increases as the value of reduction ratio (R) increases especially it increases rapidly when the value 'R' approaches certain critical value, which varies with the value of '$R_f$' and the observations found to be inline with the earlier findings. This critical value of R is known as the critical shear strength reduction factor '$R_c$' and is highly sensitive to the confining stress. As the value of $R_f$ increases, representing a transition from linear elastic nature to nonlinear nature, the value of critical shear strength reduction ratio decreases. The nonlinearity is also related with degree of jointing, thus for highly disturbed rocks, the critical shear strength ratio is relatively lower and vice versa.

Stability of the slope is a function of the shear strength and the development of failure strain reflects the potential failure zone of slope, the shear strain developed in the slope increases with reducing the shear strength. The shear strength dependency of the strain can also be exhibited though the confining stress dependent hyperbolic stress and strain model (Duncan-Chang, 1970). Here, the variation of initial tangent modulus ($E_i$) with confining stress $\sigma_3$ are represented by equations of the following form (Janbu 1963),

$$E_i = K\,Pa\left(\frac{\sigma_3}{Pa}\right)^n \tag{3}$$

K = Modulus number (dimensionless number); n = modulus exponent (dimensionless number); Pa = atmospheric pressure introduced into the equation to make conversion from one system of units to another.

The instantaneous tangent modulus is expressed as,

$$E_t = \left[1 - \frac{R_f(1-\sin\phi)(\sigma_1-\sigma_3)}{2c\cos\phi + 2\sigma_3\sin\phi}\right]^2 K\,Pa\left(\frac{\sigma_3}{Pa}\right)^n \tag{4}$$

This equation may be used to calculate the approximate value of tangent modulus for any stress condtion '$\sigma_3$' and $(\sigma_3 - \sigma_3)$ if the values of the parameters modulus number (K), modulus exponent (n), cohesion (c), angle of internal friction (ϕ) and failure ratio ($R_f$) are known. The strain can now be calculated as,

$$\varepsilon = \frac{\sigma_1 - \sigma_3}{E_i\left[1 - \frac{R_f(\sigma_1-\sigma_3)(1-\sin\phi_r)}{(2c_r\cos\phi_r + 2\sigma_3\sin\phi_r)}\right]^2} \tag{5}$$

Where, ε is the axial strain, $\sigma_1$ the major principal stress, $\sigma_3$ the minor principal stress, $R_f$ the failure ratio, $E_i$ the initial tangent modulus defined in equation 3. The $c_r$ and $\phi_r$ the reduced shear strength parameters, which are defined as,

$$c_r = \frac{c}{R} \quad \text{and} \quad \tan\phi_r = \frac{\tan\phi}{R} \tag{6}$$

where, $c$ and $\phi$ are the shear strength parameters 'R' the shear strength reduction ratio.

Here, the failure ratio ($R_f$) is the ratio of the ultimate deviatoric stress to the asymptotic value, and is the measure of the shape of stress strain curve, given as,

$$R_f = \frac{(\sigma_1 - \sigma_3)_f}{(\sigma_1 - \sigma_3)_{ult}} \tag{7}$$

$R_f$ ranges between 0 and 1, and plays a very important role in strength and deformation behaviour, specially where failure is a concern like slopes.

The critical slip surface for a slope may be found based on the equivalent plastic strain and it usually passes through the points at which the equivalent plastic strain takes the maximum in the vertical direction (Zheng et al., 2009). The equivalent plastic strain mathematically may be defined as,

$$\bar{\varepsilon}_P = \sum \Delta\bar{\varepsilon}_P\,,\ \ \Delta\bar{\varepsilon}_P = \left[(\Delta\varepsilon_P)^T(\Delta\varepsilon_P)\right]^{1/2} \tag{8}$$

Where, $\Delta\varepsilon_P$ is incremental plastic strain vector in a load step and the sum is performed with regard to all load steps. The concept of failure ratio is incorporated in shear strength reduction technique and is applied to a slope using *FLAC*. The separate large scale slope in rockmass is considered using *FLAC* for the analysis and the adopted hyperbolic model parameters are given in Table 3. Figure 6 shows the relationship between the shear strength reduction ratio 'R' and axial strain 'ε', for different values of '$R_f$'. From figure 6, it is clear that the value of 'ε' increases, as the value of 'R' increases, especially it increases rapidly when the value 'R' approaches certain critical value, which varies with the value of '$R_f$'. This critical value of 'R' is known as the critical shear strength reduction factor $R_c$ (Matsui and San 1992). This $R_c$ is also equal to the factor of safety when total shear strain is used, a factor by which if we divide the shear strength, the slope will come to verge of failure. The different critical values of shear strength ratio 'R' for different values of '$R_f$' and their variation can also be understood from Fig.7. It can be observed, a sharp decrease of critical shear strength reduction ratio with the increase of failure ratio. From the Figs. 6 and 7, it is clear that as the value of $R_f$ increases i.e., when there is transition from linear elastic nature to nonlinear nature, the value of critical shear strength reduction ratio decreases. As the nonlinearity also related with degree of jointing, and, therefore, in case of highly jointed/disturbed rocks the critical shear strength reduction ratio is relatively lower and vice versa. It can also be observed that the critical shear strength reduction ratio, $R_c$ is highly sensitive to the confining pressure and with little increase in confining stress, $R_c$ values increases rapidly as depicted in the Fig.8. This also supports the confining pressure effects on jointed rocks (Asef and Reddish, 2002) i.e. a little confining pressure actually reduces the effect of jointing and there is significant increase in the value of the critical shear strength reduction ratio.

**Table 3.** Properties used for strength dependency analysis

| Parameter | Value |
|---|---|
| K | 32500 |
| n | 0.21 |
| $R_f$ | 0.9 |
| Cohesion | 546 kPa |
| Friction | 22° |

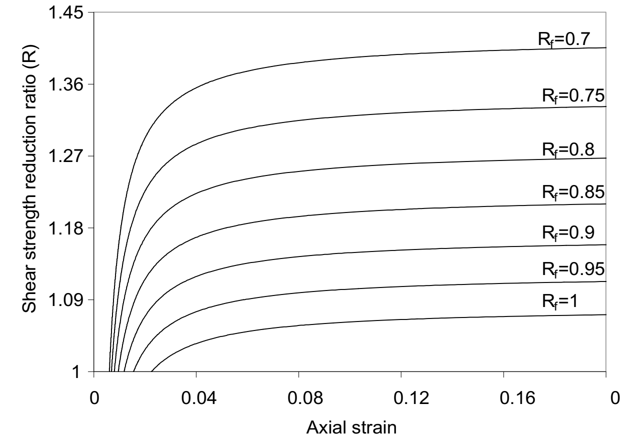


**Fig.6.** R vs ε for different $R_f$ values

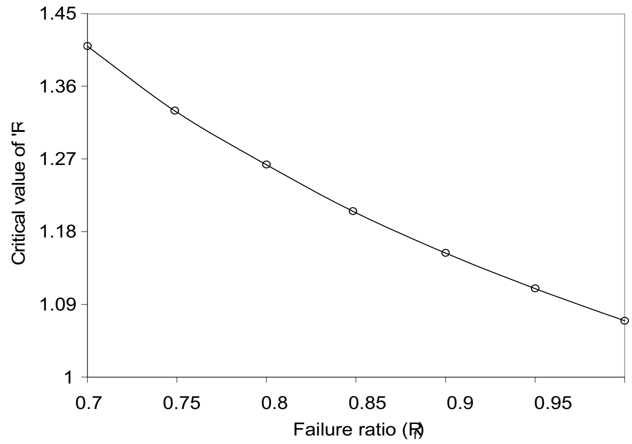


**Fig.7.** Variation of critical value of R with failure ratio $R_f$

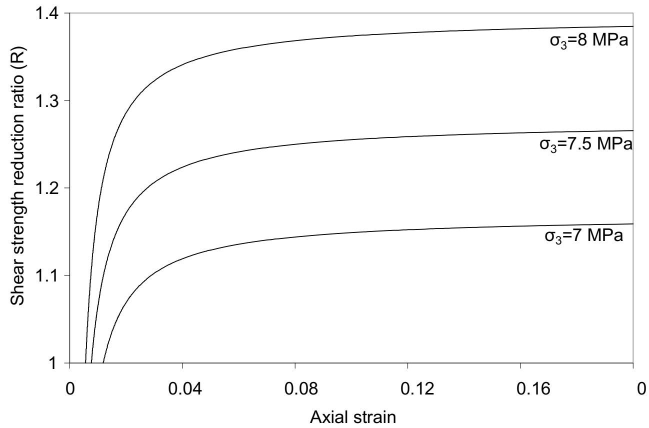


**Fig.8.** R vs ε for different $\sigma_3$ values

## CRITICAL SSR '$R_C$' AND SAFETY FACTOR

Relationships between the critical shear strength reduction ratio and the safety factor are also examined. Figure 9 shows the shear strain increment (SSI) values of the slope corresponding to different values of 'R'. The analysis started with R=1.1 and the values of R was gradually increased, i.e. the shear strength was reduced. As R increased to 1.2, a well defined failure shear zone developed from the toe to the top of the slope. This critical value of the shear strength reduction ratio ($R_c$=1.2) approximately agree with the safety factor calculated for the same slope using limit equilibrium method. It has been observed that the value of $R_c$ of the slope increases with reducing the value of $R_f$. For the present case, corresponding to $R_f$= 0.95 , $R_c$ value is found to be 1.11 , where as, with $R_f$= 0.75 the value increased to 1.33. Due

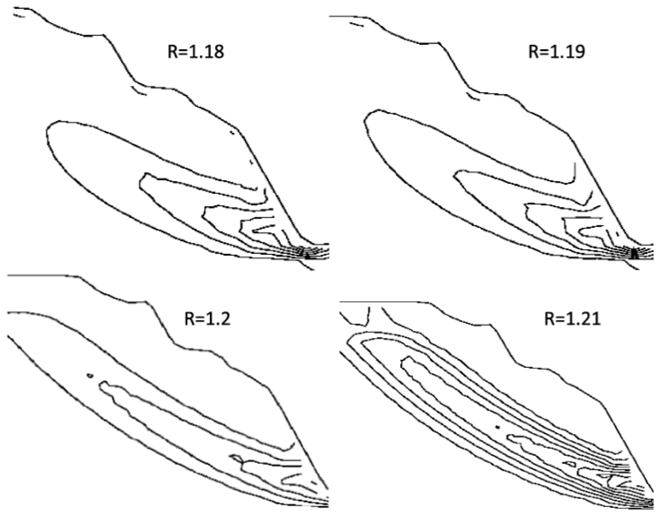


**Fig.9.** The shear strain increment distribution with different values of R

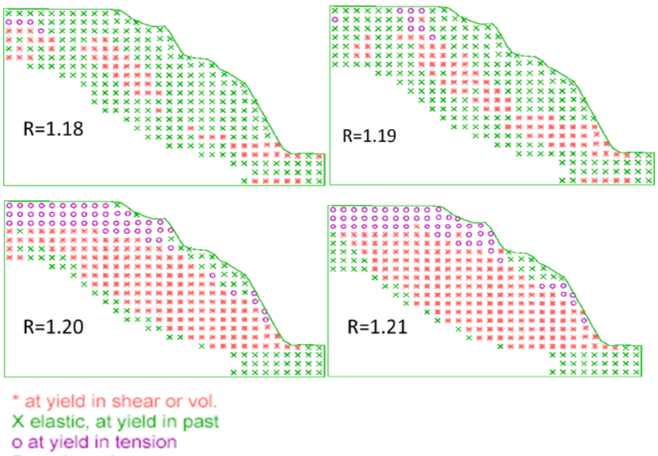


**Fig.10.** Plasticity indicator plots for different values of R

to uncertainty in the initial shear strains, only shear strain increment developed due to the slope excavation is considered. As observed, shear strain increment increases as the value of R increases. From these results, it can be concluded that the failure patterns of slopes can be successfully traced by using the shear strength reduction technique. Yielding may be understood using the plasticity indicator plot for different values of R. They reveal those zones in which the stresses satisfy the yield criterion (Fig.10). $R_c$ corresponds to the factor of safety if the total shear strain is used in the analysis. Because of the initial uncertainties of shear strain values in the slope, $R_c$ may not always be taken as the safety factor of the slope. In that case, the factor of safety for the slope can be calculated from the local safety factors along the failure surface SSR technique.

## SUMMARY AND CONCLUSIONS

Being very intuitive and straight forward, shear strength reduction (SSR) technique has become preferred choice for slope stability analysis. The manual effort involved in calculating the reduced material properties for multiple factor of safety values is fully automated in commercial softwares. The limit equilibrium and SSR results usually found to be comparable, but in case they vary a lot, care and engineering judgement is required for assessing proper solution. Cross reference of one for the other is always good for confidence. The accuracy of the solution greatly depend upon the field evaluation of the shear strength characteristics of the materials. The shear strain developed in the slope found to increase with the reduction in the shear strength and is reflected in the present analysis. The concept of failure ratio ($R_f$) is incorporated in shear strength reduction technique and is demonstrated using an example. Relationships between the critical shear strength reduction ratio and the safety factor are also examined. The critical value of the shear strength reduction ratio is a good indicator of factor of safety when total shear strain is considered but because of the uncertainties in the initial shear strain values, careful consideration is needed. The value found to be highly sensitive to the confining stress condition.

## References

Asef, M.R. and Reddish, D.J. (2002) The impact of confining stress on the rock deformation modulus. Geotechnique, v.52, pp.235-241.

Cala, M. and Flisiak, J. (2003) Slope stability analysis with numerical and limit equilibrium methods. In: Burczynski, Fedelinski & Majchrzak (Eds.) Computer Methods in Mechanics, CMM-2003.

Cheng, Y.M., Lansivaara, T. and Wei, W.B. (2007) Two-dimensional slope stability analysis by limit equilibrium and strength reduction method. Computers and Geotechnique, v.34, pp.137-150.

Dawson, E.M., Roth, W.H. and Drescher, A. (1999) Slope stability analysis by strength reduction. Geotechnique, v.49, pp.835-840.

Donald, I.B. and Giam, S.K. (1988) Application of the nodal displacement method to slope stability analysis, Proceedings of the 5th Australia-New Zealand Conference on Geomechanics, Sydney, Australia, Aug. 22-26.

Duncan, J.M. and Chang, C.Y. (1970) Non-linear analysis of stress and strain in soil. Jour. Soil Mechanics and Foundation Engg., ASCE, v.5, pp.1629-1652.

Duncan, J.M., 1996, State of the art: limit equilibrium and finite-element analysis of slopes. Jour. Geotechnical and Geoenvironmental Engg., ASCE, v.122, pp.577-596.

Griffiths, D.V. and Lane, P.A. (1999) Slope stability analysis by finite elements. Geotechnique, v.49, pp.387-403.

Itasca Consulting Group Inc. (2001) Fast Lagrangian Analysis of Continua, *FLAC* Version 4, User's Manuals.

Janbu, N. (1963) Soil compressibility as Determined by Oedometer and Triaxial tests, European Conference on Soil mechanics and Foundation Engg., Wiesbaden, Germany, 1, pp.19-25.

Kainthola, A., Singh, P.K., Wasnik, A.B., Sazid, M. and Singh, T.N. (2012) Finite element analysis of road cut slopes using Hoek & Brown failure criterion, IJEE, v.5(5) pp.1100-1109.

Lechman, J.B. and Griffiths, D.V. (2000) Analysis of the progression of failure of earth slopes by finite elements. Slope stability proceedings of sessions of Geo-Denver, Aug.5–8.

Maji, V. B. (2008) Strength and deformation behaviour of jointed rocks, Ph.D thesis, Indian Institute of Science, Bangalore, 253p.

Maji, V.B. and Sitharam, T.G. (2010) Stability of slope based on shear strain criterion and its dependency on shear strength, EUROCK Proceedings, EPFL, Switzerland, June 15-18.

Matsui, T. and San, K.C. (1992) Finite element slope stability analysis by shear strength reduction technique. Soils and Found., v.32, pp.59–70.

Naylor, D.J. (1981) Finite elements and slope stability, Numerical methods in Geomechanics, proceedings of the NATO advanced study institute, Lisbon, Portugal, pp.229-244.

Roscoe, K.H., 1970, The influence of strains in soil mechanics. Tenth Rankine lecture, Geotechnique, v.20, pp.129-170.

Singh, P.K., Wasnik, A.B., Kainthola, A., Sazid, M., Singh, T.N. (2013) The stability of road cut cliff face along SH-121- A case study, Natural Hazard, v.68(2), pp.497-507.

Ugai, K. and Leshchinsky, D. (1995) 3-dimensional limit equilibrium and finite element analyses: A comparison of results. Soils and Found., v.35, pp.1-7.

Ugai, K. (1989) A method of calculation of total factor of safety of slopes by elasto-plastic FEM, Soils and Foundations, v.29, pp.190-195.

Zheng, H., Sun, G. and Liu, D. (2009) A practical procedure for searching critical slip surface of slopes based on the strength reduction. Computers & Geotechnique, Elsevier, v.36, pp.1–6.

Zheng, Y.R., Zhao, S.Y., Kong, W.X., and Deng, C.J. (2005) Geotechnical engineering limit analysis using Finite Element Method. Rock and Soil Mechanics, v.26, pp.163-168.

Zienkiewicz, O.C., Humpheson, C. and Lewis, R.W. (1975) Associated and non-associated viscoplasticity in soil mechanics. Geotechnique, v.25, pp.671-689.

*(Received: 4 November 2015; Revised form accepted: 5 March 2016)*